

On-Beamline Calibration of the MCCDX System

Takashi KUMASAKA¹⁾, Masaki YAMAMOTO¹⁾, Kazumichi SATO¹⁾,
Tatzuo UEKI²⁾, Hidenori TOYOKAWA²⁾, and Masayo SUZUKI²⁾

1) SPring-8/RIKEN, 2) SPring-8/JASRI

1. Introduction

This report attempts to summarize the research activity undertaken during the current year regarding the "on-beamline" calibration for the Multiple CCD X-ray Detector (hereafter abbreviated as MCCDX), which has been installed into the RIKEN beamline I of the SPring-8 facility for protein crystallography. As already described in detail [1], the kernel structure of the MCCDX is a 4×4 matrix of fiber optic tapers (FOTs), each element of the FOT matrix coupled to a scientific charge-coupled-device (CCD) at its small end. When compared with other existing FOT-CCD-based X-ray detectors, the MCCDX system has the largest X-ray detection area of $200 \text{ mm} \times 200 \text{ mm}$ with a relatively low demagnification factor of 2.2 under rather moderate operation temperature of 273 K.

In order to guarantee the quality of X-ray diffraction data, however, the background noise, the image distortion and the nonuniformity in X-ray sensitivity that the MCCDX system inherently possesses must be precisely measured and adequately corrected. It almost exclusively requires "on-beamline calibration" of the system and the questions are reduced to (i) how to realize a flood-field of X-rays at the vicinity of the detector installed and (ii) how to realize a calibration mask to be attached to the detector window for this purpose.

Concerning the X-ray flood-field generation, the emission of characteristic X-rays has been regarded as one of the most promising approaches towards this technical matter, since they are known to isotropically irradiate [2]. Regarding the calibration mask pattern, a bronze plate with coating layer of Au becomes one of the best candidates, since two-dimensionally-distributing holes can be formed on this material by using photochemical etching process with an accuracy better than $20 \mu\text{m}$, having a sufficiently high X-ray absorption. As described below, these approaches have been experimentally studied during the course of establishing the "on-beamline calibration procedure" for the MCCDX system.

2. X-ray Flood-field Generation

As a novel detector of the RIKEN beamline I, the MCCDX has been located on an optical stage for X-ray crystallography (Huber 5103) together with a

diffractometer and a goniometer in the protein crystallography station [3]. The distance between the goniometer and the MCCDX, *i.e.*, the camera length, was set to be 22 cm in the present work. The materials mounted on the goniometer as characteristic X-ray radiators included sheets of gold, platinum, copper and so on. Among these various materials with different thicknesses, a zinc sheet of $25 \mu\text{m}$ in thickness was found to be the best in reference to the intensity of the characteristic X-rays generated and the spectral proximity of the characteristic X-rays generated to the energy region of interest.

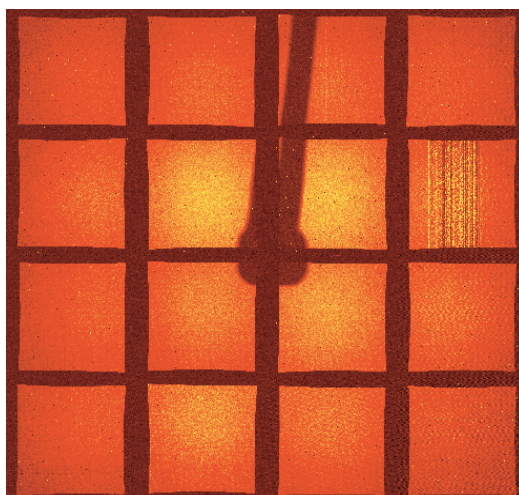


Fig. 1. An observed image of the flood-field generated by the characteristic X-rays from a zinc sheet.

Figure 1 displays a typical image observed for the flood-field thus generated. It can be seen from this figure that the flood-field radiated wide enough to cover the entire region of the X-ray sensitive area of the MCCDX. The profile of the observed flood-field image may be better seen with the gray value histogram in 3D plot shown in Fig. 2. The global structure having a maximum intensity at the central region can be naturally attributed to the fact that the solid angle subtended by a given CCD pixel at the radiator position decreases as the radial distance of the pixel increases with respect to the X-ray beam axis.

One may realize that almost a half of the active image region appearing in the second row from the top on the most-right column has been disturbed by

vertically running noise pattern, of which cause was identified with one of the electric receptacles mechanically damaged. Also there exist several pixels indicating substantially high pixel values, which look like "spikes" in Fig. 2. Since they distribute randomly in space and time, it is conceivable that they are originated from local radioactivity and/or cosmic rays.

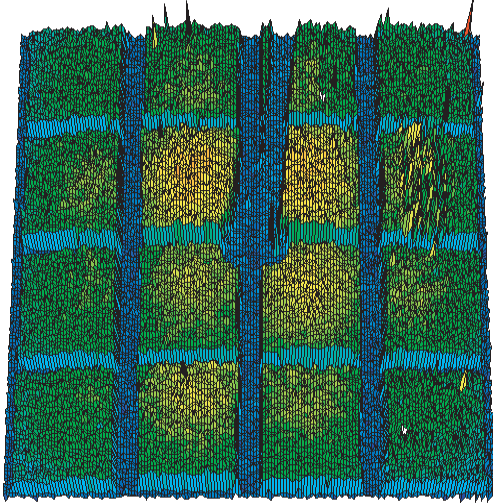


Fig. 2. Gray value histogram for the flood-field image in 3D plot.

3. Phosphor-bronze-plate Calibration Pattern

In order to configure a calibration pattern, an array of holes was made on a phosphor-bronze-plate with photochemical etching technique. The plate itself has horizontal and vertical extensions of 250 mm \times 250 mm with a thickness of 100 μ m, of which surfaces were coated with Au of 5 μ m in thickness. The holes of 150 μ m in diameter were formed with an interval of 1.0 mm in both directions over the area of 210 mm \times 210 mm on the plate. The location tolerance on center-to-center of the holes was specified at \pm 20 μ m. With horizontal and vertical intervals of 50 mm, there are 16 spatial locations on the mask where holes are missing for the purpose of measuring the relative orientations of the 16 FOT-CCD X-ray detector modules. After forming the holes, the plate was sandwiched with a pair of aluminum frames to maintain its shape, and then was attached to the MCCDX entrance window.

A part of the X-ray mask pattern image observed under the irradiation of the flood field described above and its gray value histogram in 3D plot are shown in Figs. 3 and 4, respectively. The interval and the FWHM for these peaks observed in this particular case are 1.1 mm and 200 μ m, respectively, both values being appreciably larger than those mechanically determined. The major sources of making these discrepancies are believed to be the divergence of the

characteristic X-rays, *i.e.*, parallax error. This observation simply confirms and emphasizes the needs of on-site calibrations since any X-ray diffraction data acquired with a similar system will be subject to the same effect.

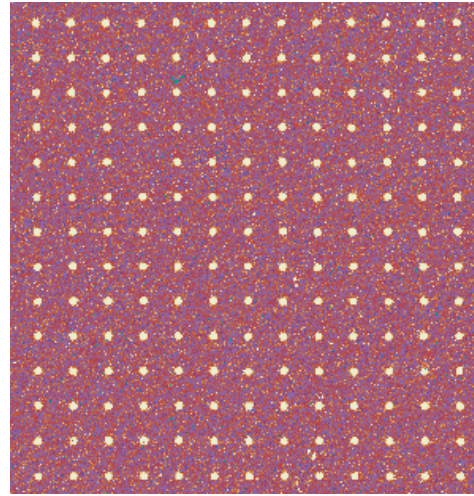


Fig. 3. A portion of the X-ray image observed with a phosphor-bronze-plate calibration mask pattern. One of the missing holes can be seen near the left top corner.

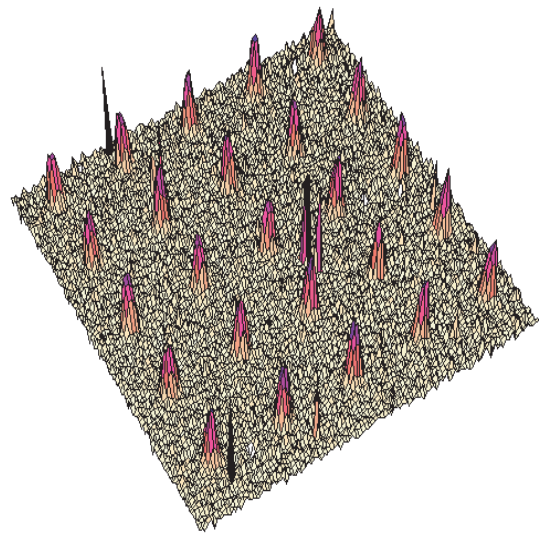


Fig. 4. Gray value histogram of the calibration mask X-ray image in 3D plot.

4. Concluding Remarks

Following the flood-field and mask pattern measurements, 60 diffraction images of a zinc protease crystal [space group: P4(3)2(1)2, crystal parameter: $a = 78 \text{ \AA}$, $c = 81 \text{ \AA}$] were acquired with an oscillation angle an X-ray wavelength of 1.5 deg and 1.28 \AA , respectively. A magnified image of the diffraction pattern observed in the present work is displayed in Fig. 5. It should be, however, noticed here that only background subtraction has been made in the diffraction image presented in Fig. 5. As stated

at the beginning of the report, accurate corrections of the nonuniformity and of the distortion must be carried out based upon the calibration data of which statistical and systematic errors are highly minimized. An intensive data analysis on a large number of calibration data that had been taken during the current year is currently under way to establish a reliable data table for the M CCDX system calibration on the beamline.

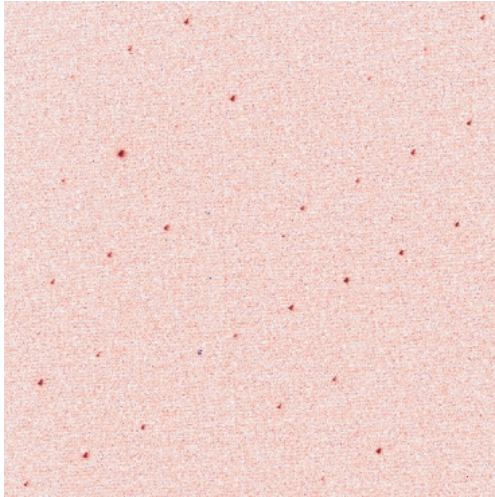


Fig. 5. A magnified X-ray diffraction image observed of a zinc protease crystal.

References

- [1] M. Suzuki, *et al.*, "A multiple-CCD X-ray detectors and its basic characterization", *J. Synchrotron Rad.* **6** (1999) 6-18.
- [2] J. P. Moy, *et al.*, "A novel technique for accurate intensity calibration of area X-ray detectors at almost arbitrary energy", *J. Synchrotron Rad.* **3** (1996), 1-5.
- [3] M. Suzuki *et al.*, "A multiple CCD X-ray detector and its first operation with synchrotron radiation X-ray beam", (1999) accepted for publication in *Nucl. Instrum. and Methods Section A*.